Shape, polarizability, and metallicity in silicon clusters

K. A. Jackson,[1] M. Yang,[1] I. Chaudhuri,[2] and Th. Frauenheim[2]
[1]*Department of Physics, Central Michigan University, Mt. Pleasant, Michigan 48859, USA*
[2]*Theoretische Physik, Universität Paderborn, D33095 Paderborn, Germany*
(Received 7 October 2004; published 30 March 2005)

We compute the dipole polarizability for Si_n clusters across the prolate to compact shape transition region, $n=20-28$, and also for a prolate and compact isomer at $n=50$. We find a clear shape dependence in the calculated values, with prolate structures having systematically larger polarizabilities, and very different trends in per atom polarizabilities with cluster size. The shape dependence is not due to highest unoccupied molecular orbital (HOMO)-lowest unoccupied molecular orbital gap differences or to differences in the binding of the HOMO electron. Instead, charge density analyses show a metalliclike response of the clusters to an external field. In addition, the size trends for the calculated polarizabilities for the compact and prolate clusters are reproduced by the predictions of jellium models for spheres and cylinders, respectively, further suggesting that these small clusters exhibit metallic character.

DOI: 10.1103/PhysRevA.71.033205 PACS number(s): 36.40.Mr, 36.40.Wa, 36.40.Qv, 61.46.+w

I. INTRODUCTION

The electric polarizability, α, measures the response of an atomic cluster to a static external electric field. It is, therefore, a useful quantity for assessing the potential behavior of clusters in nanotechnology applications. It is also a fundamentally interesting property that cannot be extrapolated easily from the behavior of corresponding bulk material, since the presence of the cluster surface typically makes the bonding in clusters very different from that in the bulk. In Si clusters (Si_n), for example, bond lengths are systematically shorter than in crystalline silicon (c-Si) and average coordination numbers are larger. In this latter respect, clusters are more similar to liquid silicon (ℓ-Si), which has a coordination number in excess of six [1], than to the four-fold coordinated, sp^3 packing in c-Si. The fact that ℓ-Si is metallic, while c-Si is semiconducting, raises the possibility that Si clusters may also exhibit metallic behavior in response to external fields.

Of added interest in the case of Si_n is the dependence of α on the overall cluster shape. Ion mobility measurements [2,3] indicate that silicon clusters, beginning at ten atoms, become more prolate with increasing size up to around $n=25$, whereupon they make an abrupt change to a compact quasispherical shape for larger sizes. It is reasonable to expect that this shape change would have a clear signature in the electronic properties of the clusters, including α.

There have been a number of theoretical studies of Si cluster polarizability [4–10]. Most of these focus on small clusters, for which the ground state structures are well known [11]. Vasiliev *et al.* [5] performed the first systematic study of α (in this paper, α refers to one-third of the per atom trace of the cluster polarizability tensor, unless otherwise noted) for $n=1-10$, using a pseudopotential-based method and the local density approximation (LDA). They found that the polarizability of the small clusters is significantly greater than the bulk limit of 3.7 $Å^3$/atom, inferred from the bulk dielectric constant using the Clausius–Mossotti relation [5], and that its value decreases smoothly over this size range. Jackson *et al.* [6] extended the range to $n=20$ by computing α for structures found in the genetic algorithm search of Ho *et al.* [12]. They found that α increases between $n=10$ and 20 and attributed the increase in part to the growing prolateness of the clusters. On this basis, these authors also predicted that the polarizability would show a shape-dependent decrease across the prolate to compact shape transition. Later, Deng *et al.* [7] found polarizabilities over the range $n=10-28$, using prolate structures constructed [12] by hand for $n>20$. These authors also found α to increase from a local minimum near $n=10$, climbing as the clusters became more prolate [7]. Because they only studied prolate structures, they did not address the change in polarizability across the shape transition.

These calculated results can be contrasted with the experimental data of Schäfer *et al.* [13]. While the calculations find large values of α for small clusters and a relatively smooth variation with cluster size, the experiments find much smaller values in general, and dramatic changes with size. Motivated by this apparent disagreement, Bazterra *et al.* [8] and Maroulis *et al.* [9,10] also studied the small clusters, carefully investigating the effect of different levels of theory (including quantum chemistry versus density functional-based approaches), different basis sets, and different choices of cluster structure on the calculated polarizabilities. The results showed that such differences in methodology have a relatively small effect on α. For example, density functional and quantum chemistry results using comparable basis sets agree to within about 1% for Si_4 [9]. Thus, differences between theory and experiment cannot be due to methodological issues.

A significant barrier to extending the polarizability calculations to larger clusters lies in first finding the appropriate ground state structures. This is a very complex problem for clusters containing more than ten atoms. Recently, we conducted extensive searches [14,15] that yielded the lowest-energy prolate and compact structures for Si_n in the $n=19-28$ atom size range. These structures correctly reproduce all known experimental data for cation and neutral clusters, including the prolate to compact shape transition at n

=25. Using the same search algorithm, we have also found a low-energy compact structure for $n=50$.

These new structures present an opportunity to probe the evolution of α for realistic geometries over a wide size range and to examine the shape dependence in the $n=20-28$ atom size range where prolate and compact structures are nearly degenerate. In this paper, we present calculated polarizabilities for these new structures and use the results to explore the shape dependence in α and to characterize cluster size trends for both prolate and compact isomers.

II. METHOD

The calculations were done using the same finite field methodology employed in our previous work [6]. We used density functional theory in the generalized gradient approximation (GGA) of Perdew, Burke, and Ernzerhof [16], as implemented in the NRLMOL program [17]. The Gaussian orbital basis set used for each Si atom was constructed from 16 Gaussian exponents, contracted to seven *s*-type, six *p*-type, and four *d*-type orbitals. The longest-ranged function of each orbital type had an exponent of 0.05396.

The electric polarizability for an atomic cluster is defined as

$$\alpha_{ij} = \left. \frac{d\mu_i}{dF_j} \right|_{F_j=0}, \tag{1}$$

where μ_i is the ith component of the cluster dipole moment and F_j is the jth component of an external electric field. The derivative can be evaluated by finite differences using the results of independent self-consistent calculations run with and without a uniform static external electric field. If F_j is a small field,

$$\alpha_{ij} = \frac{\mu_i(F_j) - \mu_i(-F_j)}{2F_j}, \tag{2}$$

where $\mu_i(F_j)$ is the dipole moment obtained in the presence of F_j. A magnitude $F_j=0.005$ atomic units yields converged results for the derivatives. We carry out independent calculations with F in the $\pm x$, y, and z directions to evaluate all the tensor components. The self-consistency criterion for the total energy was set at 10^{-7} Hartree, to ensure accurate values of μ. As mentioned above, we report results for the average polarizability per atom for the clusters, i.e., $\alpha=(1/3n)(\alpha_{xx}+\alpha_{yy}+\alpha_{zz})$, where n is the number of atoms in the cluster.

III. RESULTS

Figure 1 shows the lowest energy compact and prolate Si_n isomers found in our extensive searches for the global minima for $n=20-28$ [14,15], along with their cohesive energies (in eV atom). The prolate structures can be described as stacks of stable subunits. The prolate Si_{26} structure, for example, consists of two ten-atom units, joined by a central six-atom ring. The compact structures have no corresponding growth pattern.

As shown in the figure, the cohesive energy is larger for the prolate structures until $n=26$, whereupon compact structures become more stable. For the corresponding cation clusters, the transition in stability occurs at $n=25$, in agreement with the shape transition observed in ion mobility measurements [3]. Comparisons of computed and measured ion mobilities and cluster dissociation energies are also in excellent agreement for the cations [15], providing strong evidence that the cation structures obtained in the search are the same as those present in the experiments. Since the neutral isomers were obtained with the same search methodology, we assume that the structures in Fig. 1 are the global minima for Si_n with $n=20-28$.

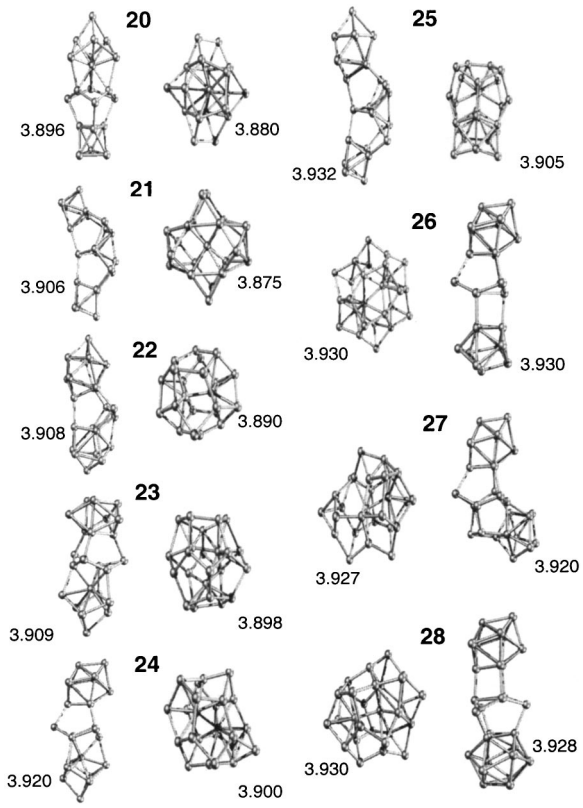

FIG. 1. Lowest-energy prolate and compact Si_n structures found in Ref. [15]. The cohesive energy in eV atom is given for each structure. It can be seen that the cohesive energy is larger for the prolate isomers until $n=26$, whereupon the compact isomers become more stable.

In Fig. 2, we show one prolate and one compact isomer for $n=50$. The compact structure is the lowest-energy structure found in an extensive ground state search using the method of Ref. [15]. While it has not been proven to be the ground state, the structure is certainly low in energy and therefore physically reasonable. Because they are relatively higher in energy for $n>26$, prolate structures do not emerge from ground state searches at $n=50$. Instead, the structure shown in Fig. 2 was constructed by joining two prolate $n=26$ isomers, removing a single cap atom from each before joining them. Since it is formed from stable subunits, we also expect this structure to be physically reasonable.

We focus first on the properties of the clusters in the $n=20-28$ size range, over which prolate and compact structures are nearly degenerate. There are clear systematic differ-

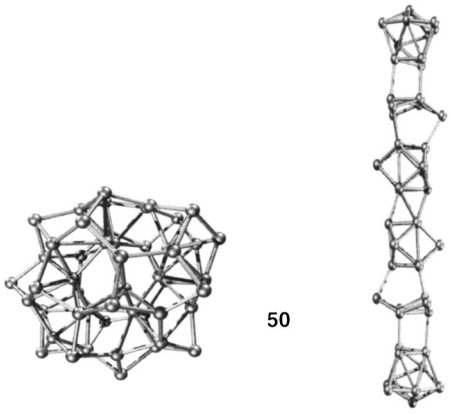

FIG. 2. Prolate and compact structures for $n=50$. The compact structure was obtained using the search method of Ref. [15]. The prolate structure was formed by joining two low-energy Si_{26} isomers, and removing a single cap atom from each.

ences in the electronic properties of the two cluster types, as shown in Table I. The highest occupied molecular orbital (HOMO)-lowest unoccupied molecular orbital (LUMO) gap, E_g, is larger for the prolate than for compact clusters at every size. The average value is 1.34 eV for the prolate clusters and 0.70 eV for compact. For comparison, the bulk Si band gap within the GGA is about 0.65 eV [18]. The value of ε_H, the HOMO energy level, is deeper for the prolate structures, implying that the HOMO electron is more strongly bound in the prolate than in the compact structures. The average value for the prolate structures is −5.31 eV, compared to −4.93 eV for compact. This difference coincides well with the fact that the compact structures have smaller ionization energies than the prolate [19]. This has the effect of making compact cation clusters somewhat more stable than prolate cations, relative to the corresponding neutrals, and accounts for the slight shift in the shape transition threshold to $n=25$ from $n=26$ in the cation clusters.

The cluster dipole moments, μ, are also given in Table I. The values are generally larger for the prolate structures, reflecting a separation of charge along the long dimension of these clusters. This occurs because of differences in the effective electronegativities of the different subunits stacked along the prolate axis. In Si_{26}, for example, the lower Si_{10} unit has a net charge of roughly $+0.1e$, the central six-atom ring a net charge of $-0.1e$, and the top Si_{10} unit is approximately neutral. The dipole moments are very small for most of the compact clusters.

The cluster polarizabilities, α, are also larger for the prolate structures than for the compact. The typical difference at each size over the $n=20-28$ range amounts to roughly 10% of the prolate value.

The prolate/compact differences in HOMO-LUMO gap, ε_h, μ, and α occur not only for the lowest-energy isomers, but for higher-lying isomers as well. Therefore, the differences can be clearly associated with overall cluster shape.

As was true for the smaller clusters, there is a general lack of agreement between the polarizabilities given in Table I and the experimental values of Schäfer *et al.* [13]. Again, the experimental values are generally much smaller and show much larger fluctuations with cluster size, between values of about 2.5 Å^3 per atom for $n=25$ and about 4.5 Å^3 per atom for $n=23$, with an average value of about 3.5 Å^3 over the range $n=20-28$ [13]. The computed values in Table I lie in the range from 4.5 to 5.13 Å^3 per atom, with an average value of 4.8. Note that since the clusters have nonzero dipole moments, an additional term, $\mu^2/3kT$, should be added to the expression in Eq. (1) to give the effective polarizability seen in experiments. This would increase the calculated values beyond those reported in Table I, particularly for the prolate clusters, increasing the disagreement between theory and experiment.

IV. DISCUSSION

It is interesting to consider the origin of the shape dependence in α seen in Table I. We note first that the prolate/compact differences cannot be explained on the basis of the HOMO-LUMO gap, E_g, or the HOMO binding energy, ε_H. A simple perturbation theory argument [5] holds that α should

TABLE I. Calculated HOMO-LUMO gap (E_g), HOMO level (ε_H), dipole moment (μ), and average per atom polarizability (α) for the lowest-energy prolate (P) and compact (C) Si_n clusters with $n=20-28$. The structures for these clusters are shown in Fig. 1.

	E_g (eV)		ε_H (eV)		μ (Debye)		α (Å^3 atom)	
N	P	C	P	C	P	C	P	C
20	1.78	0.96	−5.31	−5.14	0.53	0.41	4.93	4.59
21	1.68	1.02	−5.44	−5.09	0.55	0.03	5.09	4.68
22	1.18	0.64	−5.25	−4.95	1.25	0.07	4.86	4.54
23	1.19	0.64	−5.50	−4.93	1.13	0.32	4.99	4.51
24	1.71	0.85	−5.36	−4.93	0.62	0.21	4.97	4.55
25	1.47	0.45	−5.41	−4.65	0.76	0.18	5.13	4.60
26	1.32	0.42	−5.33	−4.87	1.10	0.53	5.09	4.70
27	1.12	0.73	−5.20	−4.93	1.11	0.53	5.06	4.64
28	0.96	0.60	−4.93	−4.90	0.13	0.75	5.03	4.57

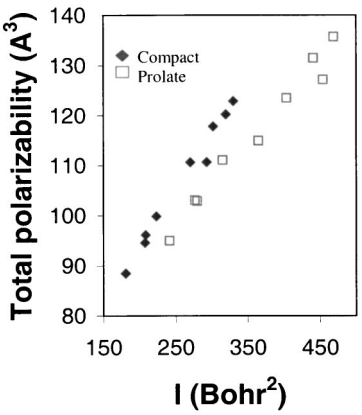

FIG. 3. Total cluster polarizability for Si_n vs $I=\Sigma_{i=1}^{n} r_i^2$ for the clusters in Fig. 1. Here, r_i is the distance of atom i from the cluster center of mass. Filled diamonds represent compact clusters and open squares prolate.

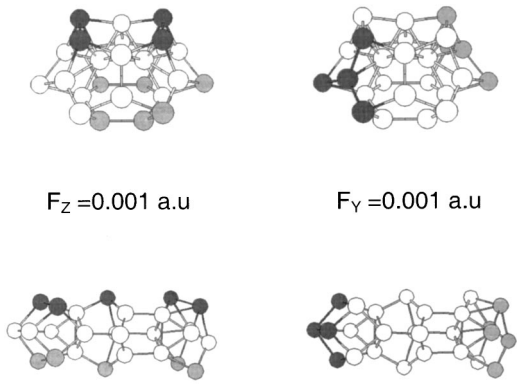

FIG. 4. Charge transfer caused by applying the indicated static uniform external electric field to the prolate and compact isomers for Si_{26}. The shading indicates atoms that have gained or lost more than $0.02e$. Light gray atoms have lost charge, while dark gray atoms have gained charge.

be inversely related to E_g, but in Table I prolate clusters can be seen to have both larger gaps and larger values of α at each cluser size. Furthermore, clusters with more tightly bound valence electrons might be expected to be less polarizable, suggesting that that ε_H should be inversely related to α, but again the results in Table I show that the opposite is true for prolate and compact clusters. The shape dependence must therefore go beyond these differences in electronic structure.

Deng *et al.* [7] took a different approach to modeling the shape dependence, studying the relationship between the *total* cluster polarizability and a simple geometrical parameter, $I=\Sigma_{i=1}^{n} r_i^2$, where r_i is the distance of atom i to the cluster center of mass. I increases relatively faster for prolate than for compact clusters and could, therefore, explain the increase in α with prolateness. In Fig. 3, we plot the total polarizabilities versus I for the prolate and compact clusters with $n=20-28$. The figure indeed shows a correlation between I and α, but the correlation is clearly different for the two cluster shapes. The shape dependence is clearly more complicated than the difference in I between clusters.

An alternative approach to understanding the shape dependence begins by examining the effect of an external electric field on the distribution of charge in the clusters. To do this, we divide space into a collection of atomic volumes, analogous to Wigner–Seitz zones in periodic systems. The volume for a given atom is that region of space geometrically closer to the chosen atom than to any other in the cluster. The atomic charge, q_i is the integral of the total charge density within the corresponding atomic volume. It is a straightforward matter to define the atomic volumes and to compute q_i using the numerical integration mesh in NRLMOL [17].

Changes in the charge distribution related to an external field can be visualized by comparing atomic charges calculated with and without the field. In Fig. 4, we show $\delta q_i = q_i(F_j) - q_i(0)$, for a magnitude $|F_j|=0.001$ a.u. in two perpendicular field directions for both prolate and compact $n=26$ isomers. Shading is used to indicate atoms that gain or lose more than $0.02e$ as a result of the external field. The largest value of δq in both clusters is approximately $0.09e$.

The charge transfer depicted in Fig. 4 shows a metal-like pattern in both clusters, as the external field drives electron charge from one side of the cluster to the other, while the net charge on the interior atoms remains approximately constant. Summing over the surface atoms, we find a net charge transfer in the range of 0.20 to $0.28e$ for the compact cluster depending on the field orientation, and 0.20 to $0.25e$ for the prolate structure.

The metalliclike distributions shown in Fig. 4 suggest that size trends in the polarizability could be understood using models appropriate for metallic systems. The jellium model [20,21] assumes that electrons move in the potential of a uniform positive background charge, mimicking the effective potential seen by conduction electrons in a metal. Using self-consistent LDA calculations, Beck [22] found that the polarizability of a jellium sphere can be expressed as:

$$\alpha = (r + \delta)^3, \tag{3}$$

where r is the radius of the positive background charge and δ is the so-called spill-out parameter, simply interpreted as the distance the electronic density extends beyond the background positive charge. Guan *et al.* [23] recast this equation to model the results for Na_n clusters, expressing the sphere radius in terms of the atomic number density, ρ:

$$\alpha/n = \left[\left(\frac{3}{4\pi\rho}\right)^{1/3} + \frac{\delta}{n^{1/3}}\right]^3. \tag{4}$$

Using our calculated value of α for the Si atom, 5.98 Å^3, and the bulk limit $\alpha=3.71$ Å^3, we can fit the two parameters in this equation, ρ and δ, yielding $\rho=6.43\times10^{22}$ cm^{-3}, which corresponds to a mass density of 2.99 g/cm^3, and $\delta=0.278$ Å. These values can be compared to the analogous quantities for ℓ-Si, which has a density of 2.59 g/cm^3 at $T=1800$ K [1] and an average bond length of 2.55 Å, estimated from the pair correlation function given in Ref. [1]. The average bond length in Si clusters at 0 K is about 2.45 Å. Scaling the ℓ-Si density by $(2.55/2.45)^3$ yields 2.92 g/cm^3, within about 2% of the result of the fit, showing

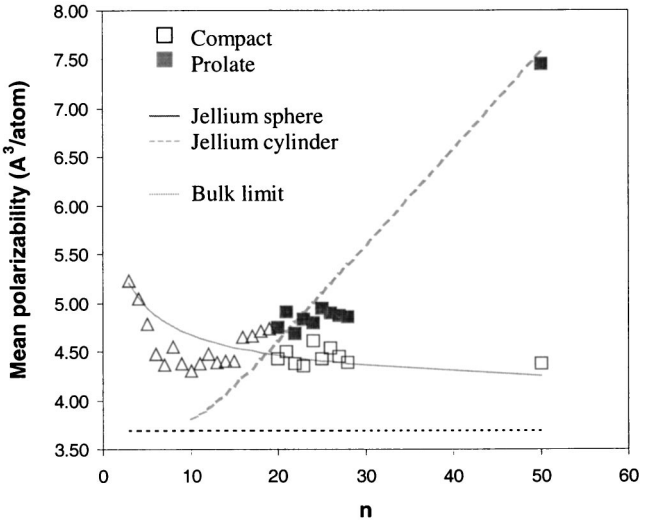

FIG. 5. Trends in the per atom average polarizability for Si_n. The filled squares are for prolate clusters and the open squares compact ($n=20-28$). The open triangles are calculated values obtained for the ground state clusters with $n<20$. These become increasingly prolate over the range $n=10-19$. The solid line is the prediction of Eq. (4), the jellium sphere model [24]. The dashed line is the prediction of Eq. (5), the jellium cylinder model [18].

that the fit value is physically reasonable for a metallic Si structure at low temperature.

The value for δ from the fit is about 11% of the cluster bond length, a reasonable value giving its spill-out interpretation. This is somewhat smaller than the roughly 25% ratio found for Na_n [18]. The difference may reflect stronger binding of the electrons in Si_n.

The prediction of Eq. (4) is plotted in Fig. 5 along with the first-principles values of α. The latter show significant variation from the model, especially for smaller cluster sizes, but the model fits the overall cluster size trend for the compact clusters (open squares) very well, including the value for $n=50$. The slight decrease with size is due to the diminishing impact of the spill-out radius, which becomes a smaller fraction of the overall cluster radius with increasing size.

For the prolate clusters, we turn to a model described by Apell *et al.* [24] for jellium cylinders. The model was originally developed to treat the energy deposition of fast ions in materials, taking into account effects due to the shape and geometry of the target molecules. Combining expressions for the average excitation energy of a jellium system with sum rules for oscillator strengths and the polarizability, they derived an expression for the average polarizability, of a cluster:

$$\alpha = \frac{V}{v(\beta)}, \tag{5}$$

where V is the cluster volume, and v is a depolarization factor that depends only on the cluster shape. For a jellium cylinder,

$$v = \frac{2}{\beta}\int_0^\infty (1-e^{-\beta t})\left(\frac{J_1(t)}{t}\right)^2 dt \tag{6}$$

where $\beta=L/R$, L is the cylinder length, and R is its radius.

Measuring directly from Fig. 4 and assuming the boundary for the jellium background to extend one-half a bond length beyond the centers of the outermost atoms, we find $R=3.68$ Å and $L=15.0$ Å for the prolate Si_{26} isomer. We use the same value of R for the remaining prolate clusters, since all are constructed from similar subunits. The cylinder length in (Å) can then be given as $L=(15.0/26)n$, since the cluster volume scales linearly with n and is proportional to L.

The results of the jellium cylinder model are also plotted in Fig. 5. The model underestimates the calculated polarizabilities near $n=10$ but reproduces the general increasing trend for prolate clusters (filled squares). Particularly striking is the fact that the model extrapolates nearly perfectly to the calculated value for the $n=50$ prolate structure. The relative failure of the model at the smaller sizes is likely due to the assumption of cylindrical geometries. This description is crude at the smaller sizes where the clusters are more nearly spherical, but becomes increasingly apt for the larger clusters [25].

Figure 5 shows that jellium models reproduce both the magnitude and the cluster size trends of α for both the prolate and compact clusters over the intermediate size range, suggesting that the clusters display a metal-like response to a static field. This result can be understood in qualitative terms by appealing to the structural similarities between clusters and ℓ-Si, which is metallic [1]. The clusters in Figs. 1 and 2 feature average coordination numbers for all atoms of approximately 4.5 for both prolate and compact structures. The values for interior atoms are naturally larger than for atoms on the surface. In the compact Si_{26} structure, for example, the two interior atoms are seven-fold coordinated. For comparison, the coordination number for atoms in ℓ-Si, obtained by integrating the radial distribution function out to its first minimum, is about 6.4 [1]. In these highly coordinated structures, the bonding combines covalent and metallic character, resulting in a nonzero density of states at the Fermi level in the case of ℓ-Si, and the metallic response seen in Fig. 5 in the clusters.

V. SUMMARY

In this paper, we have used the structures obtained in a recent ground state search for Si_n [15] to investigate the shape dependence of cluster electronic properties. We find prolate clusters to have systematically larger HOMO-LUMO gaps, dipole moments, and polarizabilities than compact clusters across the range $n=20-28$. By also including results for prolate and compact isomers for $n=50$, we explore the shape-dependent trends with size for both cluster types. In Fig. 5, we see that the per atom polarizability for compact structures decreases slowly with size toward the bulk limit, whereas prolate clusters become increasingly polarizable. Both trends are captured very well by jellium-based models of the polarizability, suggesting that the response of these

clusters to a static external field is metallic, a conclusion that is reinforced by an analysis of charge transfers in the clusters due to an external field, as shown in Fig. 2.

It is clear from Figs. 1 and 2 that subnanometer silicon clusters have not yet evolved the sp^3 bonding pattern of *c*-Si. It remains a fascinating problem to determine the size range over which these bulklike features emerge and how the physical properties of the clusters will change as this occurs. We are currently working to address such questions.

ACKNOWLEDGMENT

This work was supported in part by DOE Grant No. DE-FG02-03ER15489.

[1] I. Stich, R. Car, and M. Parrinello, Phys. Rev. Lett. **63**, 2240 (1989).
[2] M. F. Jarrold and V. A. Constant, Phys. Rev. Lett. **67**, 2994 (1991).
[3] R. R. Hudgins, M. Imai, and M. F. Jarrold, J. Chem. Phys. **111**, 7865 (1999).
[4] K. A. Jackson, M. R. Pederson, D. Porezag, Z. Hajnal and Th. Frauenheim, Phys. Rev. B **55**, 2549 (1997).
[5] I. Vasiliev, S. Ögüt, and J. R. Chelikowsky, Phys. Rev. Lett. **78**, 4805 (1997).
[6] K. A. Jackson, M. R. Pederson, C.-Z. Wang, and K. M. Ho, Phys. Rev. A **59**, 3685 (1999).
[7] K. Deng, J. Yang, and C. T. Chan, Phys. Rev. A **61**, 025201 (2000).
[8] V. E. Bazterra, M. C. Caputo, and M. B. Ferraro, J. Chem. Phys. **117**, 11158 (2002).
[9] G. Maroulis and C. Pouchan, Phys. Chem. Chem. Phys. **5**, 1992 (2003).
[10] G. Maroulis, D. Begue, and C. Pouchan, J. Chem. Phys. **119**, 794 (2003).
[11] K. Raghavachari and C. M. Rohlfing, J. Chem. Phys. **89**, 2219 (1988).
[12] K. M. Ho *et al.*, Nature (London) **392**, 582 (1998).
[13] R. Schäfer, S. Schlecht, J. Woenckhaus, and J. A. Becker, Phys. Rev. Lett. **76**, 471 (1996).
[14] I. Rata, A. A. Shvartsburg, M. Horoi, Th. Frauenheim, K. W. M. Siu, and K. A. Jackson, Phys. Rev. Lett. **85**, 546 (2000).
[15] K. A. Jackson, M. Horoi, I. Chaudhuri, Th. Frauenheim, and A. A. Shvartsburg, Phys. Rev. Lett. **93**, 013401 (2004).
[16] J. P. Perdew, K. Burke, and M. Ernzerhof, Phys. Rev. Lett. **77**, 3865 (1996).
[17] M. R. Pederson and K. A. Jackson, Phys. Rev. B **41**, 7453 (1990); K. A. Jackson and M. R. Pederson, *ibid.* **42**, 3276 (1990).
[18] Y.-M. Juan, E. Kaxiras, and R. G. Gordon, Phys. Rev. B **51**, 9521 (1995).
[19] K. A. Jackson (unpublished).
[20] M. Brack, Rev. Mod. Phys. **65**, 677 (1993).
[21] W. A. de Heer, Rev. Mod. Phys. **65**, 611 (1993).
[22] D. E. Beck, Phys. Rev. B **30**, 6935 (1984).
[23] J. Guan, M. E. Casida, A. M. Köster, and D. R. Salahub, Phys. Rev. B **52**, 2184 (1995).
[24] S. P. Apell, J. R. Sabin, S. B. Trickey, and J. Oddershede, Int. J. Quantum Chem. **86**, 35 (2002).
[25] A polarizability model for jellium ellipsoids was also presented in Ref. [24]. Because an ellipsoid with the same volume and maximum cross section is more prolate than a cylinder, the ellipsoid model predicts α to increase significantly faster with cluster size than the cylinder model. The prolate clusters in Fig. 1 have an approximately constant cross section and are thus are better described as cylinders.